

Freeze-drying as a novel concentrating method for wastewater detection of SARS-CoV-2

Rui Dong^a, Elizabeth Noriega Landa^a, Hugues Ouellet^b, Wen-Yee Lee^a, Chuan Xiao^{a*}

^aDepartment of Chemistry and Biochemistry, The University of Texas at El Paso, 500 W. University Ave, El Paso, TX 79902, USA

^bDepartment of Biological Sciences, The University of Texas at El Paso, 500 W. University Ave, El Paso, TX 79902, USA

Abstract

Extracting and detecting viral RNA in wastewater has proven to be a rapid and cost-effective approach for community-level monitoring during the recent global Severe Acute Respiratory Syndrome Coronavirus 2 (SARS-CoV-2) pandemic. Various sample concentrating methods, such as centrifugal ultrafiltration, have been utilized in wastewater SARS-CoV-2 detection studies. However, freeze drying, a promising technique commonly used for concentrating and preserving various biological samples, has yet to be explored in this field. This study compared the performance of freeze-drying and the widely used centrifugal ultrafiltration method in terms of recovery rate, detection limit, and other key parameters for concentrating 72 wastewater samples collected from four facilities in El Paso, TX. Statistical analyses revealed that the freeze-drying method demonstrated higher overall recovery efficiency (20.33% vs 13.00%), a superior detection ratio (68.4% vs. 31.6%), and lower detection limits (0.06copies/mL vs 0.35copies/mL) than centrifugal ultrafiltration, particularly during the early stages of the pandemic. Despite its longer processing time than centrifugal ultrafiltration, freeze-drying offers several notable advantages, including eliminating pretreatment steps, providing flexible sample storage options, preventing signal loss and sample degradation, and reducing labor and exposure risks. Freeze-drying also does not require intensive training for concentrating sewage water. These benefits, combined with its efficient capture of viral RNA, position freeze-drying as a promising alternative for wastewater virus detection, especially in resource-constrained lab settings at local wastewater treatment plants. The protocol and findings reported here provide a baseline for further development of freeze-drying-based methods for enabling community-level early warning and surveillance against emerging viral threats in the future.

Keywords: wastewater; viral RNA detection; SARS-CoV-2; concentrating; freeze-drying; centrifugal ultrafiltration.

* Corresponding Author. Tel.: +01-915-747-8657

Email Address: cxiao@utep.edu

1. Introduction

Coronavirus disease 2019 (COVID-19) is caused by the Severe Acute Respiratory Syndrome Coronavirus 2 (SARS-CoV-2), a single-stranded RNA virus. The World Health Organization has classified COVID-19 as a global pandemic. As of December 15, 2024, the total number of deaths attributed to the disease worldwide is 7,079,142 (CDC, 2020b; World Health Organization, 2020). To proactively monitor and mitigate the further dissemination of the virus at the early stage of a pandemic, the surveillance of viral presence in wastewater has emerged as a significant strategy. Notably, in March 2020, Medema et. al., conducted the first-ever successful research in the Netherlands, highlighting the feasibility of wastewater-based surveillance for COVID-19 (Medema et al., 2020). Subsequently, Wurtzer et. al. detected viral genetic material in wastewater samples before the epidemic reached a massive scale around March 8th (Wurtzer et al., 2020). Furthermore, Fontenele et. al. screened SARS-CoV-2 viral signals from 91 wastewater samples among 11 states (Fontenele et al., 2021). Quantifying of SARS-CoV-2 viral RNA in sewage offers the possibility to develop an early alarm system, providing valuable insights into disease prevalence and potential virus transmission within populations. A similar system can provide early alarm for future pandemics, allowing public health authorities more time to respond. Thus, a sensitive and cost-effective method will be desirable for such applications.

46 Nevertheless, assessing viral load within wastewater presents challenges due to the variable composition of
47 sewage. Wastewater comprises both liquid and solid phases, each containing a variety of substances (Wakefield,
48 2015). The liquid phase primarily consists of water with dissolved substances, including organic and inorganic
49 compounds, nutrients, and pathogens (Friedler et al., 2013; Henze, 2008; Prot et al., 2022; Shi et al., 2021; Zhang et
50 al., 2021). The solid phase includes suspended solids, colloidal particles, and settleable materials based on their size
51 and behavior in water (Otterpohl and Buzie, 2013; Rashid et al., 2021; Sahu et al., 2014). Moreover, the composition
52 of wastewater is influenced by numerous factors, including local precipitation, drought conditions, temperature
53 fluctuations, and water usage patterns (Hughes et al., 2021). Therefore, the concentration of viruses in wastewater
54 can fluctuate widely. In addition, nuclease in the environment can potentially degrade viral nucleic acids,
55 particularly RNA, representing another significant factor impacting RNA viral concentration in wastewater (Farkas
56 et al., 2020). Considering all these variables, detecting minute quantities of specific pathogens in the complex matrix
57 of wastewater represents a substantial challenge, necessitating proper sample handling to ensure the collection and
58 preservation of viruses for subsequent detection.

59 To tackle these challenges, the detection method should be developed specifically to address the properties
60 of wastewater. Such a method should efficiently collect viruses from both phases of wastewater while safeguarding
61 the viral genomic materials from degradation. It is crucial to maintain appropriate temperatures during sample
62 handling and minimize the processing time to prevent RNA degradation due to the ubiquitous existence of RNase in
63 the environment (Farkas et al., 2020). Given the expected low viral load during the early stages of a pandemic and
64 the fluctuation of viral concentration in wastewater, a substantial volume of samples is required to achieve
65 detectable results. In addition, sampling at multiple sites and time points is required for such an early warning
66 system to work. Thus, an efficient concentrating method that is safe and minimizes labor-intensive processes is
67 highly desirable for long term surveillance. The U.S. Centers for Disease Control and Prevention (CDC) have
68 outlined five distinct methodologies for concentrating viral particles from wastewater: ultrafiltration, electronegative
69 membrane filtration with sample pre-treatment, polyethylene glycol (PEG) precipitation, skim milk flocculation, and
70 centrifugal ultrafiltration. While each of these methods employs different principles to address the challenge of low
71 viral RNA content in wastewater, none fully meets all the criteria for effectively concentrating and detecting viruses.
72 Filtration-based methods are limited to collecting viruses in the liquid phase, potentially missing those associated
73 with solid particles. The use of additional chemicals in electronegative membrane filtration, precipitation, and
74 flocculation potentially inhibits subsequent viral detection. Ultracentrifugation cannot handle large-volume
75 samples, limiting its practicality for widespread usage. In summary, achieving sensitive viral RNA detection in
76 wastewater samples, especially during the onset or decline of COVID-19 peaks with sporadic infections,
77 necessitates the development of more strategic sample concentrating methods.

78 A promising yet unexplored approach in concentrating wastewater is freeze-drying. Traditionally, this
79 technique has been widely used to preserve various biological products in laboratory and industry circumstances
80 (Liu and Zhou, 2015). It has also been utilized for environmental samples, such as soil, to preserve and concentrate
81 nucleic acids for next-generation sequencing (Weißbecker et al., 2017). Recently, freeze-drying was used to
82 concentrate wastewater samples to evaluate the deactivating effect of Fe³⁺ treatment on bacteria (Qin et al., 2018).
83 However, freeze-drying has not been explored for virus detection in wastewater. During freeze drying, ice within
84 samples is sublimated into vapor under vacuum and frozen temperature conditions, effectively removing water from
85 wastewater matrices. This method uniquely retains viral entities from both the liquid and solid components of
86 wastewater, potentially enhancing detection sensitivity. Additionally, freeze-drying does not rely on reagent-
87 dependent sample pre-treatment, thus preserving sample integrity from chemical interventions. The cryogenic
88 environment during freeze-drying prevents the degradation of viral RNA, thereby increasing the detection limit in
89 the subsequent steps. Although the overall processing time for large-volume samples is lengthy, freeze drying offers
90 operational convenience by requiring minimal human oversight after initial setup. In summary, freeze drying is an
91 ideal choice for sensitive, reliable, and less labor-intensive virus detection methodologies, as it minimizes viral loss
92 and optimizes the protection of viral RNA.

93 This study will be the first to apply freeze drying to measure SARS-CoV-2 levels in wastewater. A
94 comparative analysis was conducted between freeze drying and centrifugal ultrafiltration as concentrating methods
95 for wastewater samples. Throughout the subsequent sections, “ultrafiltration” will be used in lieu of the more
96 descriptive term “centrifugal ultrafiltration” to improve conciseness. Ultrafiltration was chosen for comparison
97 because it is the widely used method, having been employed in the first and several early publications on detecting
98 of SARS-CoV-2 in wastewater. In this study, factors such as recovery efficiency and detection limit were compared
99 and evaluated between these two methods using Reverse Transcription Quantitative Polymerase Chain Reaction
100 (RT-qPCR). The resulting data is pivotal for developing a sensitive, precise, reproducible, and practical system to
101 detect viruses in wastewater, ultimately enhancing community-level early warning and surveillance capabilities.
102

103 **2. Material and Methods**

104 *2.1. Sample collection and pasteurization*

105 On the designated sample collection dates, 500 mL 24-hour composite wastewater samples were obtained
106 from four wastewater treatment plants (WWTPs) in El Paso, Texas, USA. These WWTPs include Haskell Street
107 Wastewater Plant (HS), John T. Hickerson Water Reclamation Facility (JH), Fred Hervey Water Reclamation (FH),
108 and Roberto Bustamante Wastewater Plant (BU). For safety concerns during the pandemic before the person-to-
109 person transmission pathway of the SARS-CoV-2 was elucidated (March 2020 to July 2020), a sample collecting
110 protocol was developed and approved by the Institutional Biosafety Committee of the University of Texas at El
111 Paso. Individuals collecting samples wore disposable single-use nitrile gloves (double layer), splash goggles, N95
112 or surgical masks, and disposable lab coats.

113 Samples were collected in the pre-cleaned wide-mouth leak-proof bottles (Fisherbrand™, Cat# 05719709),
114 which were then capped and sealed with parafilm, and the exterior was disinfected with Cavicide using absorbent
115 pads. Both the bottle and the absorbent pads were placed into one zip-lock bag, and then in a second zip-lock bag.
116 The double zip-lock bagged samples were transferred to the non-porous hard-plastic transport cooler with coolant
117 blocks and spill-absorbing materials inside until arrival at the biosafety level 2 (BSL-2) lab. Upon sample retrieval,
118 the surface of the Ziploc bags was wiped with disinfectant one more time.

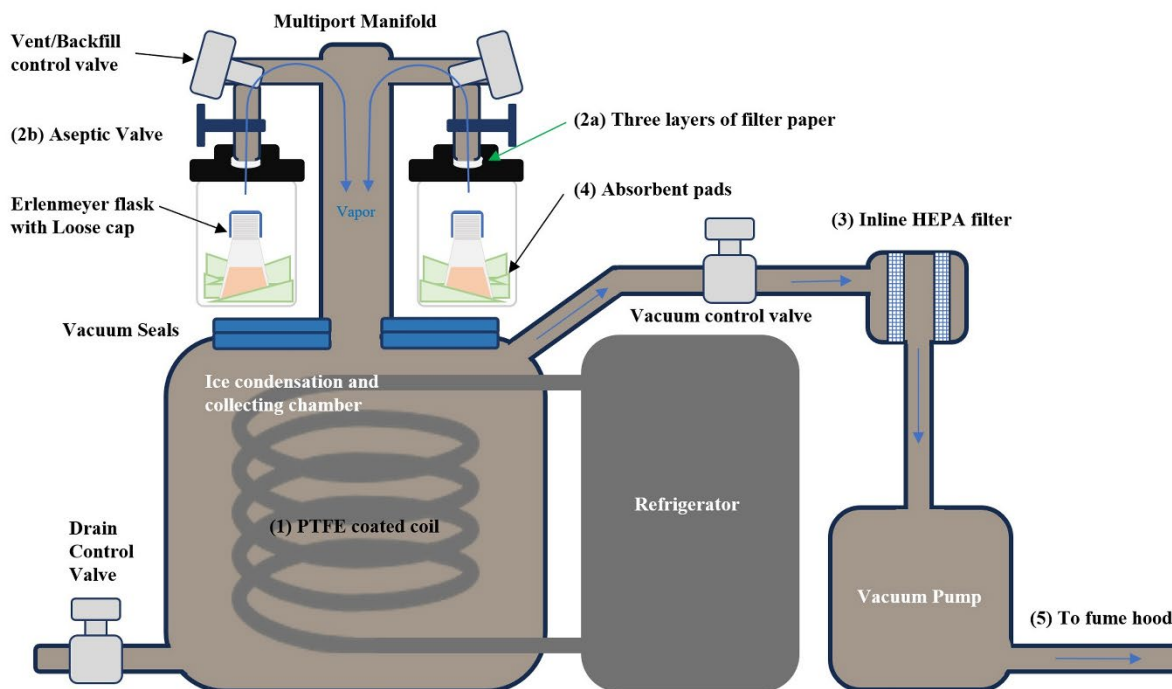
119 Samples collected in the early days of the pandemic, before the analysis protocol was fully developed, were
120 immediately frozen and stored at -80°C until further analyses. Before analyses, these early pandemic samples were
121 thawed and pasteurized in a water bath at 65°C for 90min to inactivate any remaining virus as recommended by the
122 CDC guidelines (CDC, 2020a). After the protocol was fully developed during the later period of the pandemic, the
123 collected samples were pasteurized before being stored at -80°C.

124 *2.2. Sample concentrating via freeze-drying*

125 Although samples were pasteurized and thus considered to be biosafety level 1 (BSL-1) based on the CDC
126 guidelines (CDC, 2020a), a fully sealed freeze-drying set-up was overcautiously designed and implemented using
127 FreeZone 2.5 Liter -84°C Benchtop Freeze Dryer (Labconco™, Cat# 710201000), this design is illustrated in Fig. 1.
128 The biosafety set-up incorporated multiple safeguards: (1) The freeze dryer vacuum chamber contained PTFE
129 coated coil, which is resistant to erosive disinfectants that are used after each freeze-drying cycle; (2) Three layers of
130 Filter papers (Labconco™, Cat# 7544810) and aseptic valve (Labconco™, Cat# 7543900) were added between the
131 fast-freeze flask and manifold to prevent any potential accidental pathogen from passing through; (3) A HEPE filter
132 was added before vacuum pump as the secondary filter to capture any potential accidental pathogen leakage and
133 spillage; (4) Wastewater samples were placed inside plastic Erlenmeyer flasks which were wrapped with absorbent
134 pads in 600ml Complete Fast-Freeze Flasks (Labconco™, Cat# 7540800). The absorbent pads were intended to
135 capture any accidental spill; and (5) The exhausting pipe was connected to the chemical fume hood, to exhaust the
136 odorous volatile organic compound from the wastewater. Even with these safety designs, as an extra precaution, all
137 potentially contaminated containers and the flow path before the HEPA filter were disinfected after each freeze-
138 drying run.

139 Prior to the freeze-drying procedure, 200ml of each pasteurized wastewater sample was weighed and
140 aliquoted to a 250ml plastic Erlenmeyer flask, wrapped with absorbent pads, placed into a zip-lock bag, and frozen
141 at -80°C at least overnight. On the day of concentrating, the frozen samples in Erlenmeyer flasks wrapped with
142 absorbent pads were then placed in Fast-Freeze Flasks with plastic Erlenmeyer flask caps loosened. Freeze-drying
143 was conducted with temperature set to -86°C and vacuum to 0.040mbar. After approximately three days of freeze-

144 drying, sample masses were reduced to about 3g. Volume reduction factors were estimated by sample weight before
145 and after freeze drying. The freeze-dried samples were dissolved in three volumes (v/w), approximately 9mL, of
146 TRIzol™ LS reagent (Thermo Fisher Scientific, Cat # 10296-028). Samples were vortexed to ensure thorough
147 mixing before storing at -20°C until viral RNA extractions. It has been proven that TRIzol will deactivate all viral
148 pathogens such as SARS-CoV-2 in the sample (Patterson et al., 2020). Therefore, the following steps will be
149 considered as BSL-1.
150



151
152 **Fig. 1. Schematic diagram of freeze-drying set-up.** Key biosafety safeguard features are highlighted and labeled with numbers
153 within the diagram.

154 2.3. Sample concentrating via ultrafiltration

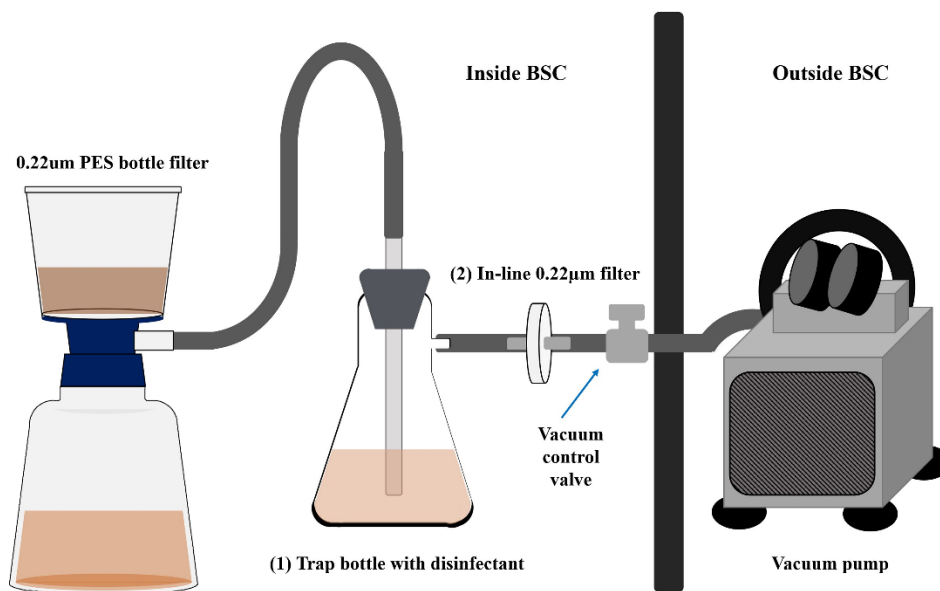
155 In parallel to concentrating samples via freeze-drying, another 200ml of pasteurized wastewater sample
156 was aliquoted into four 50ml conical tubes and loaded into swinging buckets (Thermo Fisher Scientific, Cat#
157 75003655) with adaptors (Thermo Fisher Scientific, Cat# 75003683) for the TX-400 rotor (Thermo Fisher
158 Scientific, Cat# 75003181). The swinging buckets are sealed with ClickSeal Biocontainment Lids (Thermo Fisher
159 Scientific, Cat# 75003656) and wiped with disinfectant on the outside before centrifuging at 3000×g for 15min
160 using Multifuge X1R Refrigerated Centrifuge (Thermo Fisher Scientific, Cat# 75004251). After centrifugation, the
161 supernatant was filtered using a 0.22µm PES bottle filter (Corning™, Cat# 431096) while the pellets were collected
162 and weighed. Three volumes of (v/w) TRIzol™ LS reagent was added to the weighed pellet. All these procedures
163 were carried out in a biosafety cabinet (BSC) to ensure safety. Fig. 2 illustrates the filter system with multiple,
164 overcautiously designed safeguards: (1) A trap bottle with disinfectant on the bottom was connected to the filter
165 bottle to capture any potential accidental pathogen leakage and spillage; (2) An in-line 0.22µm filter was added
166 before the vacuum valve further to capture any potential accidental pathogen leakage and spillage.

167 Inside the BSC, the filtered supernatants from the previous step were aliquoted (approximately 70ml) into
168 Centricon Plus-70 with 10kDa MW cut-off membrane (MilliporeSigma, Cat# UFC701008) and placed into
169 disinfected swinging buckets (Thermo Fisher Scientific, Cat# 75003655, with seal cap Cat# 75003656). The buckets
170 were completely sealed with ClickSeal Biocontainment Lids (Thermo Fisher Scientific, Cat# 75003656) and wiped
171 with disinfectant on the outside before being taken out from BSC to be loaded onto TX-400 rotor (Thermo Fisher
172 Scientific, Cat# 75003181). The samples were centrifuged at 3500×g for about 15min using Multifuge X1R
173 Refrigerated Centrifuge (Thermo Fisher Scientific, Cat# 75004251). After centrifugation, the swinging buckets were
174 moved back into the BSC, and the passthrough liquid was disinfected and discarded. Following the same

175 centrifugation protocol, the remaining filtered supernatants were added to Centricon Plus-70 units for the next round
176 of concentrating via ultrafiltration.

177 After three to four rounds of centrifugation, the sample volume was reduced from 200ml to approximately
178 0.5mL. Following the manufacturer's instructions, the filters were inverted and centrifuged at 1,000×g to collect the
179 concentrates. The concentrated samples were subsequently transferred to new tubes and mixed with three volumes,
180 approximately 1.5mL, of TRIzol™ LS reagent. TRIzol treated samples were vortexed to ensure thorough mixing
181 before being stored at -20°C until viral RNA extractions. Volume reduction factors for ultrafiltration were
182 determined by comparing the weights of the samples before and after concentrating. All the filters and liquid
183 transfer pipettes were soaked in ~1% bleach for at least 15min before being safely discarded.
184

184



185

186 **Fig. 2. Schematic diagram of the in-line filter system.** Key biosafety safeguard features are highlighted and
187 labeled with numbers within the diagram.

188 2.4. Viral RNA extraction and quantification

189 SARS-CoV-2 RNA was extracted and purified using the PureLink™ RNA Extraction Kit (Thermo Fisher
190 Scientific, Cat# 12183018A). Prior to RNA extraction, the frozen samples mixed with TRIzol were thawed at room
191 temperature. For every milliliter of sample mixed with TRIzol, 0.2ml of Chloroform was added. The mixture was
192 then centrifuged at 12,000×g at 4°C for 30mins using ST16 Centrifuge (Thermo Fisher Scientific, Cat# 75004381).
193 Following centrifugation, the colorless upper aqueous phase, which contains the RNA, was carefully extracted and
194 collected. Ethanol was then added to the collected sample to reach a final concentration of 35%. The samples were
195 aliquoted (600µL each) into spin cartridge provided in the kit and then spun at 6,800×g for 30s. The process of
196 aliquoting and spinning was repeated until the entire sample was passed through the spin cartridge. The bound RNA
197 was eluted from the spin cartridge in 30µL of ribonuclease-free water and collected by centrifugation. To maximize
198 RNA recovery, second and third elutions were performed by adding 100µL of ribonuclease-free water and
199 centrifuging. The purified viral RNA was immediately analyzed by one-step RT-qPCR or stored at -20°C to
200 minimize RNA degradation.

201 SARS-CoV-2 RNA was quantified by one-step RT-qPCR using N1 and N2 primers sets suggested by the
202 CDC (Dare et al., 2007; Lu et al., 2020) (Table 1). Samples were analyzed using the TaqPath™ 1-Step RT-qPCR
203 (Thermo Fisher Scientific, Cat# A15299) in 20-µL reactions. The PCR reactions were run at 50°C for 15min and
204 95 °C for 2min, followed by 45 cycles of 95°C for 5s and 55°C for 30s per manufacturer's recommendations. The
205 performance and efficiency of N1 and N2 primers in the RT-qPCR assay were first evaluated by generating standard
206 curves using ten-fold series dilution (100 to 10⁵ copies per reaction) of templates: (1) a DNA plasmid containing
207 complete nucleocapsid gene from SARS-CoV-2 (IDT, Cat# 10006625), and (2) Twist synthetic SARS-CoV-2 RNA
208 (Twist Bioscience, Cat# MT0075s44). The standard curve was plotted as RT-qPCR Ct value (y-axis) against the log
209 of copy number (x-axis) estimated from the dilution of the original standards (Fig.4). Linear least square fitting was

210 performed for each set of plotted data using the equation $y = a \times x + b$. The quality of these fittings was accessed
 211 using the coefficient of determination R^2 values. To evaluate the stabilities of DNA and RNA standards, RT-qPCR
 212 standard curves were generated the day when they were prepared and again after three or four months of storage at -
 213 20°C. Small-scale RT-qPCR was performed using a Magnetic Induction Cycler (Bio Molecular System, Cat# 71-
 214 101). Later, the StepOnePlus™ Real-Time PCR System (Thermo Fisher Scientific, Cat#4376600) was used for
 215 large-scale RT-qPCR.

216 The original DNA and RNA stock had concentrations of 2.0×10^5 copies/ μ L and 1.0×10^6 copies/mL,
 217 respectively. According to the literature, the Ct value from RT-qPCR is linear to the logarithm of sample
 218 concentration (Bustin et al., 2009). Therefore, using the 10-fold diluted standard curves, Ct values from specific RT-
 219 qPCR can be converted into virus concentration in units of copies/mL using a fitted function of the standard curve as
 220 shown in Fig.4. Then, for each elution, the amount of virus detected can be calculated using the equation:

221
 222
$$\text{Virus detected} = \text{Virus concentration} \times \text{elution volume (30}\mu\text{L for 1}^{\text{st}} \text{ elution and 100}\mu\text{L for 2}^{\text{nd}} \text{ elution)} \quad \text{Eq. 2.1}$$

223 Total copies of the virus detected (column Total copies in Supplementary Table 1) will be the summation
 224 of the virus detected from both elutions. The detecting viral concentration in the original unconcentrated sample
 225 (column D.c. in Supplementary Table 1) can be determined using the equation:

226
 227
$$\text{Detected concentration} = \text{Total copies} / \text{original sample volume} \quad \text{Eq. 2.2}$$

228 These calculations for detected concentration in the original unconcentrated sample also enable the
 229 comparison of analytical sensitivity between the two concentrating approaches. Method-specific detection limits
 230 were determined by the minimum detected concentration from all the wastewater samples using the same method
 231 (Supplementary Table 1 last row).

232
 233 Table 1 RT-qPCR primer sequences

| Assay | Primer | Sequence |
|---------------|----------------|---|
| SARS-CoV-2 N1 | Forward primer | 5'-GACCCCAAAAATCAGCGAAAT-3' |
| | Reverse primer | 5'-TCTGGTTACTGCCAGTTGAATCTG-3' |
| | Probe | 5'-FAM-ACCCCGCATTACGTTTGGTGGACC-BHQ1-3' |
| SARS-CoV-2 N2 | Forward primer | 5'-TTACAAACATTGGCCGCAAA-3' |
| | Reverse primer | 5'-GCGCGACATTCGAAGAA-3' |
| | Probe | 5'-FAM-ACAATTTGCCCCAGCGCTTCAG-BHQ1-3' |
| OC43 | Forward primer | 5'-CGATGAGGCTATTCCGACTAGGT-3' |
| | Reverse primer | 5'-CCTCCTGAGCCTCAATATAGTAACC-3' |
| | Probe | 5'-6FAM-TCCGCTGGCAGGTTACTCCCT-BHQ-3' |

234 **2.5. Recovery efficiency calculations using OC43**

235 OC43 was chosen as the surrogate virus in this study to calculate recovery efficiency for both concentrating
 236 methods: freeze-drying and ultrafiltration. To estimate the amount of virus to be spiked to wastewater for recovery
 237 efficiency calculation, a standard curve of heat-inactivated OC43 virus was generated. The virus infectivity of the
 238 original stock of heat-inactivated OC43 culture fluid (ZeptoMetrix, Cat# 0810024CFHI) is defined by the median
 239 tissue culture infectious dose (TCID₅₀), the dilution of virus required to infect 50% of the given cell monolayers (Lei
 240 et al. 2020). An exact 100 μ L aliquot of this inactivated OC43 at 5.0×10^8 TCID₅₀/ μ L was used to prepare a 10-fold
 241 serial dilutions with water. The concentration of inactivated OC43 in each dilution was determined based on the
 242 dilution factor. These serially diluted samples were then subjected to the same procedures aforementioned for
 243 TRIzol treatment, RNA extraction, and RT-qPCR, but with different primer/probe sets for OC43 (Sigma Custom
 244 DNA Oligos Cat# 41105327) (Table 1). Following a similar approach mentioned in Section 2.4 for DNA and RNA
 245 standards, a standard curve was established by plotting the RT-qPCR Ct value (y-axis) against the logarithm of heat-
 246 inactivated OC43 concentration, expressed in the units of TCID₅₀.

247 To calculate the recovery efficiency of the virus from the wastewater sample, an exact 20 μ L aliquot of
 248 Zeptomatrix heat-inactivated OC43 was spiked into 400ml wastewater sample. To demonstrate that RT-qPCR

249 cannot detect the virus without concentrating the wastewater sample, 1mL of spiked sample was collected and
250 treated with 3 mL of TRIzol™ LS reagent. The remaining spiked sample was divided into two parts (approximately
251 200mL each) and concentrated via either freeze drying or ultrafiltration, following the same procedure described in
252 Sections 2.2 and 2.3 on sample concentrating. Viral RNA was then extracted and analyzed by RT-qPCR using the
253 same procedure described previously in Section 2.4, but with a different primer/probe set for OC43 as listed in
254 Table 1.

255 Using the initial concentration (5.0×10^8 TCID₅₀/μL) and volume (20μL) of heat-inactivated virus spiked
256 into wastewater, the total amount of virus added was estimated to be 2.67×10^4 TCID₅₀/μL. After concentrating the
257 spiked wastewater sample using freeze-drying and ultrafiltration, RT-qPCR was performed on the extracted and
258 purified RNA sample using the same conditions as used for the heat-inactivated OC43 standard curve. The Ct value
259 from the RT-PCR and the standard curve allowed the estimation of the amount of virus recovered by the two
260 methods, expressed in the unit of TCID₅₀/μL. Recovery efficiency was then calculated as the ratio of the recovered
261 virus amount to the amount initially spiked, with both values expressed in units of TCID₅₀. The recovery efficiency
262 estimations were performed in triplicate, allowing for the calculating the mean and standard deviation for each
263 method. A Wilcoxon test, a nonparametric statical hypothesis test without assuming a normal distribution of the data
264 (Damian Riina et al., 2023), was subsequently conducted to determine whether there was a significant difference
265 between the two methods.

266 *2.6. Creatinine measurement*

267 Creatinine concentration was measured to evaluate human contribution to wastewater. Frozen pasteurized
268 samples were thawed at 4°C, and 100μL was aliquoted for creatinine analyses using a creatinine colorimetric
269 detection assay (Enzo Life Sciences, Cat# ADI-907-030).

270 *2.7. Epidemiological data and statistical analysis*

271 Daily COVID-19 record from April 14, 2020, to May 28, 2021 in El Paso, TX, was collected from
272 <https://www.epstrong.org/results.php> and <https://elpasocovid19tracker.com/index.html>. Sampling dates with
273 associated viral load calculations from all four wastewater plant sites are listed in Supplementary Table 1. The
274 correlation between the total COVID-19 cases and SARS-CoV-2 viral load in wastewater was evaluated using the
275 Pearson correlation coefficient (Lee Rodgers and Nicewander 1988). This correlation coefficient, ranging from -1 to
276 1, provided a quantitative measure of the observed relationship between the two variables: COVID-19 case numbers
277 and SARS-CoV-2 viral load in wastewater. A correlation coefficient close to zero means no correlation, while close
278 to 1 and -1 indicate strong positive or negative correlation, respectively. All data processing and statistical analyses
279 were conducted using R Studio (Rstudio Team, 2020).

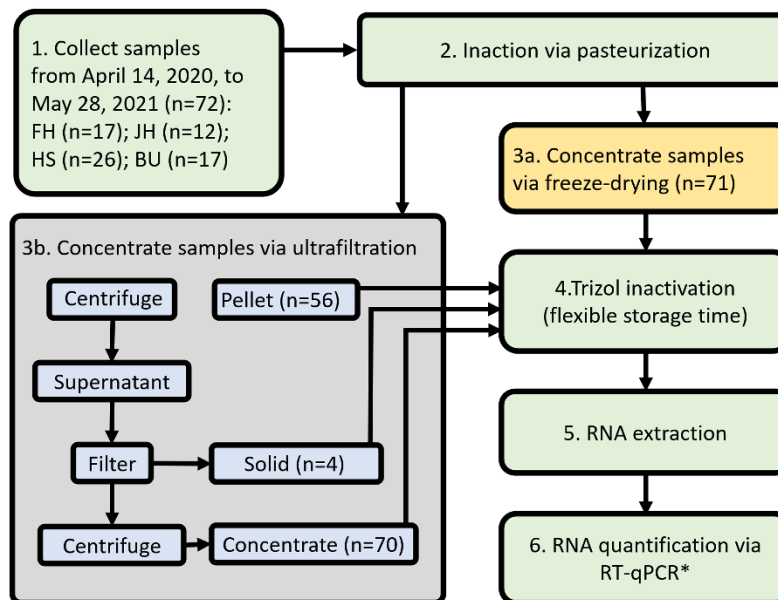
280 **3. Results and Discussion**

281 Our study underscores the importance of strict safety procedures when handling wastewater samples
282 containing emerging pathogens, particularly in adhering to the stringent biosafety standards set by institutions such
283 as the CDC and NIH. The designs of our wastewater sample collection and processing protocols reflect a strong
284 commitment to these high safety standards. A multilayer safety setup was implemented during sample collection and
285 pasteurization, including the use of disposable protective gear, rigorous disinfection protocols, and an approved
286 safety protocol developed early in the SARS-CoV-2 pandemic. This proactive approach to biosafety was crucial
287 during uncertain times. Combining sample collection with immediate pasteurization, a swift transition to BSL-1
288 became possible, offering a versatile solution for handling unknown emerging pathogens. This approach is
289 particularly beneficial for laboratories with limited resources, such as those affiliated with wastewater treatment
290 plants.

291 *3.1. Number of Samples*

292 A total of 83 wastewater samples were collected from four wastewater treatment plants (WWTPs) in El
293 Paso, Texas, USA, from April 14, 2020, to May 28, 2021. However, some samples from certain WWTPs were
294 unavailable due to technical and personnel challenges encountered during the pandemic. During the initial small
295 peak between April 2020 and May 2020, 71 samples were collected and stored in a -80°C freezer using sample
296 collection protocol approved by the Institutional Biosafety Committee (IBC) at the University of Texas at El Paso

297 (UTEP) before the analytic protocol was fully developed and approved by IBC. Due to the limited lab accessibility
298 during the pandemic, human resources constraints, and the restricted storage space in -80°C freezers, sample
299 collection was paused between August 2020 and April 2021. Once the samples were processed using the fully
300 developed and approved protocol and storage space was freed up in -80°C freezers, sample collection was resumed
301 in May 2021. The collection frequency during this period was more sporadic, depending on the processing speed of
302 stored samples. For the second period, a total of 12 samples were collected. Following pasteurization to inactivate
303 wastewater pathogens, 71 samples were concentrated using freeze-drying and 70 using ultrafiltration respectively.
304 Additionally, 56 pellets were collected from 70 ultrafiltration samples (Fig.3). Unfortunately, RT-qPCR data for
305 about 10 samples were lost due to an unexpected crash of the computer that controls the StepOnePlus™ Real-Time
306 PCR System. At the end, data from a total of 72 samples were obtained (Fig. 3, Supplementary Table 1).



308

309 **Fig. 3. Flowchart of sample processing with sample numbers.** Samples collected from four different WWTPs were inactivated through
310 pasteurization, and then concentrated using two methods. The number of samples processed at each pre-process step is indicated in parentheses
311 after "n =". Viral RNA of all the samples was extracted from concentrated samples and subjected to RT-qPCR for quantification. FH, Fred
312 Hervey Water Reclamation Plant; JH, John T. Hickerson Water Reclamation Facility; HS, Haskell R. Street Wastewater Treatment Plant, Bu,
313 Roberto Bustamante Wastewater Treatment Plant.

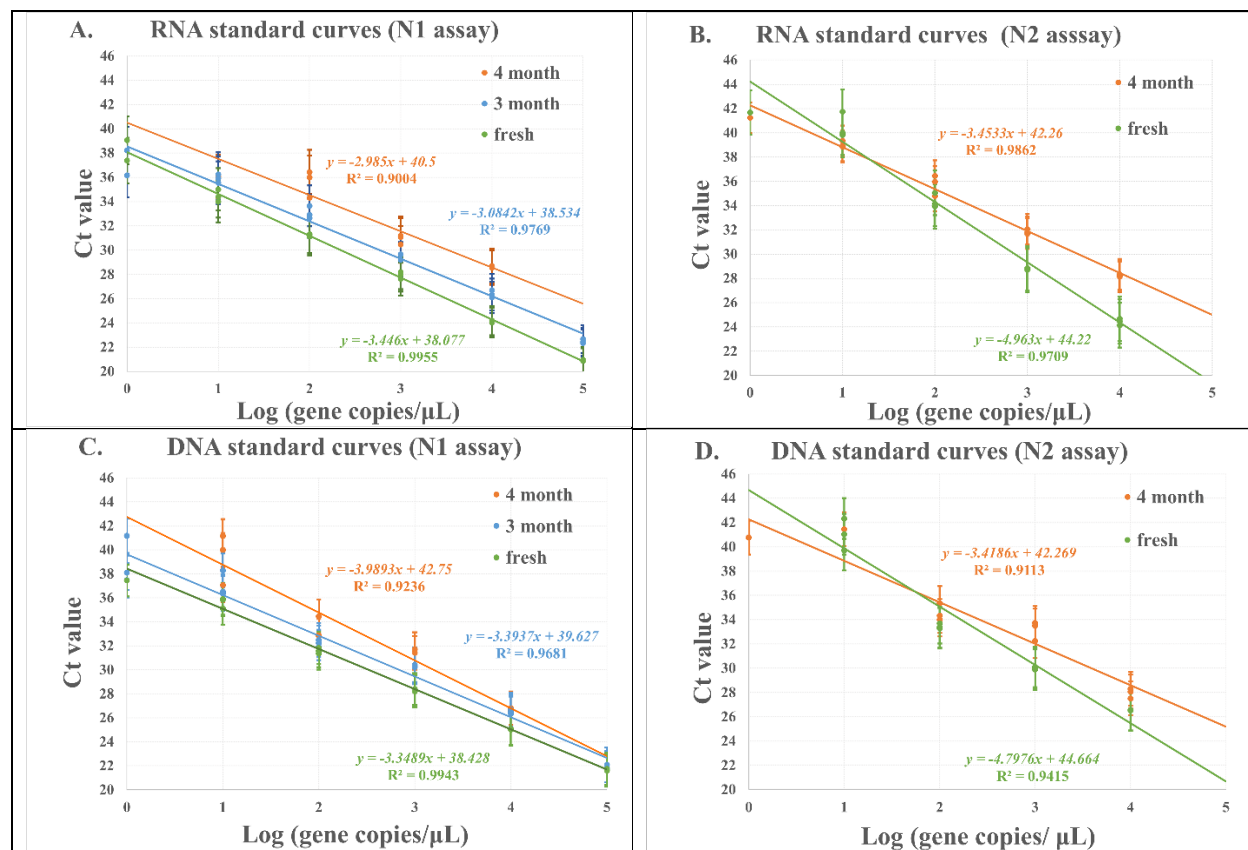
314 3.2. RT-qPCR primer selection and template stabilities

315 Fig. 4 (original data in Supplementary Table 2) shows standard curves and their least-squares regression
316 equations $y = a \times x + b$, with coefficients a and b . The slope a should be negative, with an absolute value between
317 3.3 and 3.4, as the literature suggests that each 10-fold drop of the template is expected to increase approximately 3
318 PCR cycles to reach the same fluorescent signal value (Svec et al., 2015). Any value out of this range indicates
319 potential issues with the dilution of standard templates or suboptimal RT-qPCR conditions. The y-intercept b
320 represents the Ct value when there is no template, where the fluorescence may arise from one or more of the
321 following: non-specific amplification, primer-dimer formation, and background signal (Taylor et al., 2017).

322 The standard curve analysis provides valuable insights into the performance and suitability of the N1 and
323 N2 primers for quantifying RNA and DNA targets from SARS-CoV-2 samples. Across all time points of RNA and
324 DNA standards, the N1 primer consistently exhibited higher R^2 values than the N2 primer, indicating a stronger
325 linear correlation between the measured and expected quantities. Additionally, the fitted lines of N1 for both RNA
326 and DNA are lower than those of N2, reflecting overall lower Ct values for the N1 primer. These higher R^2 values
327 and lower overall Ct values highlight the superior quantification accuracy and reliability of the N1 primer, making it
328 the preferred choice. However, the impact of standards degradation over time cannot be overlooked, as evidenced by
329 the progressive increase in the heights (Ct values) of fitting lines observed for both RNA and DNA standards.
330 Obviously, RNA exhibited more significant degradation than DNA underscoring its higher susceptibility to

331 degradation. The crossing observed in the RNA and DNA standard curves using N2 primers after storage in Fig. 4B
332 and Fig. 4D suggests that the N2 primer region may be more susceptible to degradation, resulting in deviations from
333 the expected slope (approximately -3) of the standard curve. Consequently, while the N1 primer is the optimal
334 choice for fresh samples due to its stronger linear correlation, DNA standards are more suitable for long-term studies
335 or situations requiring extended sample storage, owing to its greater stability. Therefore, for the subsequent studies,
336 we used DNA standards to estimate the total number of detected viruses.

337

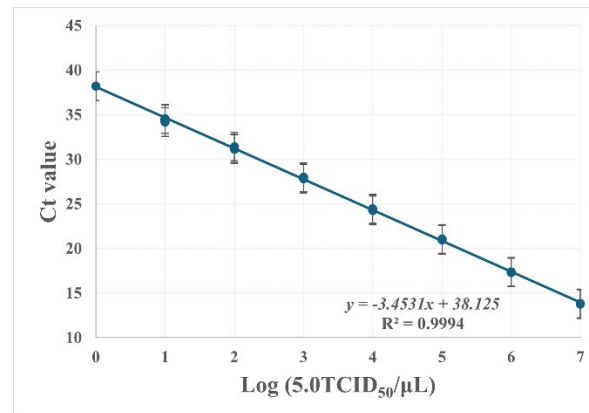


338 **Fig. 4. RNA and DNA standard curves.** Panels A and B display the fitted lines of qPCR Ct values plotted against gene copies of serially diluted
339 RNA standards, using the N1 and N2 primers, respectively. Panels C and D present similar fitted lines for DNA standards. As the legend
340 indicates, the different line colors represent standard curves generated from fresh samples or samples stored at -20°C for 3 or 4 months. The fitted
341 equations and corresponding R² values are shown in the same colors as their respective lines.

342 3.3. Comparison of recovery efficiency of two concentrating methods

343 To compare the recovery efficiency of the two concentrating methods, OC43 was spiked into a wastewater
344 sample. Both OC43 and SARS-CoV-2 are beta-coronaviruses that cause respiratory infections in humans and are
345 transmitted via droplets and/or aerosols. However, unlike SARS-CoV-2, OC43 does not cause severe disease in
346 humans, making it an ideal surrogate for laboratory recovery tests without biosafety concerns.

347



348

349 **Fig. 5. OC43 standard curve.** qPCR Ct values are plotted against gene copies in units of TCID₅₀/μL, derived from serial dilutions of OC43 RNA
 350 standards. The fitted line illustrates the relationship using specific primers targeting OC43, with the corresponding equation and R² value shown
 351 on the graph.

352 Table 2. Recovery rate of freeze-drying and ultrafiltration

| Method | Ct | Average Ct (±SD) | Recovered virus (TCID ₅₀ /μL) | Recovery rate |
|-----------------|-------------------|------------------|--|---------------|
| Freeze drying | 27.93 27.38 27.70 | 27.67 (±0.34) | 5.42 x 10 ³ | 20.33% |
| Ultrafiltration | 28.61 28.22 28.18 | 28.34 (±0.66) | 3.47 x 10 ³ | 13.00% |

353

354 Based on the standard curve using heat-inactivated OC43 virus (Fig.5, original data in Supplementary
 355 Table 3), approximately 10.0×10⁹TCID₅₀ of the virus was spiked into 400mL of wastewater. This sample was
 356 divided into two equal volumes and concentrated using either freeze-drying or ultrafiltration methods. A control
 357 sample without concentrating had an undetermined Ct value, indicating that RT-qPCR could not detect the OC43
 358 signal prior to concentrating. Recovery rates were calculated based on the Ct values from the first RNA extraction
 359 elution and were found to be 20.33% for the freeze-drying method and 13.00% for the ultrafiltration method. The
 360 freeze-drying method demonstrated a recovery efficiency that was superior to or at least comparable with the widely
 361 used ultrafiltration technique.

362 Notably, the second elution from the freeze-dried sample exhibited a lower Ct value than the first elution
 363 (Supplementary Table 1). This phenomenon was also observed in other freeze-dry concentrated wastewater samples
 364 during SARS-CoV-2 detection but not in the sample concentrated via ultrafiltration or RNA extracted from heat-
 365 inactivated OC43 serial dilution when establishing the standard curve. Since the freeze-drying process concentrates
 366 all small molecules, it is possible that inhibitory substances affecting RT-qPCR may also be enriched. When
 367 combining the recovery rates from both the first and second elutions, the overall recovery rates remained at 22.37%
 368 for freeze-drying and 13.93% for ultrafiltration, demonstrating the potential advantage of the freeze-drying
 369 approach.

370 3.4. Comparison of early detection of two concentrating methods

371 To evaluate the detection sensitivities of the freeze-drying and ultrafiltration methods, wastewater viral
 372 load data from the early stages of the COVID-19 pandemic (April 2020 to May 2020) were analyzed. A total of 38
 373 samples were collected from various wastewater treatment plants in El Paso, Texas. The freeze-drying method
 374 identified 26 positive samples (68.4%) (Table 3). As previously discussed, the freeze-drying method yielded lower
 375 Ct values (indicating more sensitive detection) in the second elution. When the second elution was included, the
 376 detection ratio increased to 28 positive samples (73.7%). In contrast, the ultrafiltration detected only 12 positive
 377 samples (31.6%), which increased slightly to 13 positive samples (34.2%) when including the second elution (Table
 378 3). The higher detection ratio observed with the freeze-drying method highlights its superior ability to concentrate
 379 viral material compared to ultrafiltration.

380
381

Table 3 Positive ratio and Ct value range for samples collected from four WWTPs between April 2020 to May 2020

| Site | Sample Number | Positive numbers | | Positive Ratio % | | Range of Ct Value | |
|-------|---------------|------------------|-----------------|------------------|-----------------|-------------------|-------------------|
| | | Freeze dry | Ultrafiltration | Freeze dry | Ultrafiltration | Freeze Dry | Ultrafiltration |
| HS | 18 | 12 (14) | 5 (6) | 66.7 (77.8) | 27.8 (33.3) | 31 (32) – 42 (42) | 33 (33) – 38 (38) |
| JH | 1 | 1 (1) | 1 (1) | 100.0 (100.0) | 100.0 (100.0) | 33 (33) – 33 (35) | 35 (35) – 36 (36) |
| FH | 8 | 6 (6) | 5 (5) | 75.0 (75.0) | 62.5 (62.5) | 32 (32) – 39 (39) | 32 (32) – 41 (41) |
| BU | 11 | 7 (7) | 1 (1) | 63.6 (63.6) | 9.1 (9.1) | 33 (33) – 37(37) | 33 (33) – 34 (34) |
| Total | 38 | 26 (28) | 12 (13) | 68.4 (73.7) | 31.6 (34.2) | | |

382 * Numbers in the parentheses are values obtained from the second elution

383

384 The superior detection sensitivity of the freeze-drying method was further supported by the lower average
 385 Ct values obtained during RT-qPCR analyses. Across all four wastewater treatment plants, the freeze-drying method
 386 consistently exhibited lower Ct values compared to ultrafiltration (Table 3), indicating a higher amount of viral RNA
 387 in the concentrated samples. Furthermore, a paired T-test analysis was conducted to compare virus copies in the
 388 original wastewater samples across all four facilities. As described in the Section 2., the total virus copies were
 389 estimated using the DNA standard curve and the Ct values. For both freeze dry and ultrafiltration methods, both first
 390 and second elutions were combined to calculate the total RNA copies in the original wastewater samples. Where a
 391 method or elution did not detect the virus, it was recorded as zero copies. A total of 11 data pairs showed that freeze-
 392 drying method detected significantly higher virus concentration than ultrafiltration with a p-value smaller than
 393 0.0068 from the Wilcoxon test. As described in Section 2.4, method-specific detection limits can be determined
 394 using the highest Ct value for each method and the standard curves. The freeze-drying method demonstrated a lower
 395 limit of detection (0.06 copies/mL) compared to ultrafiltration (0.35 copies/mL) (Supplementary Table 1).

396 3.5. Correlated virus load and case number in epidemic

397 Due to the substantial variation in wastewater flow rate caused by weather conditions (rainfall, drought, and
 398 temperature-dependent evaporation) and fluctuations in water usage throughout the day, estimating the proportion of
 399 human contribution to wastewater is challenging (Katukiza et al., 2012). To address this issue, the concentration of
 400 creatinine, a metabolic product from humans, has been proposed as an internal control for assessing human
 401 contribution to wastewater (Chen et al., 1977; Daughton, 2012). However, many of the reported creatinine levels in
 402 wastewater, as low as 0.01 mg/dL (Rusiñol et al., 2021), are close to or outside the limit of the detection kit (0.042
 403 mg/dL) (Enzo Life Sciences Cat# ADI-907-030), raising concerns about the reliability of using creatinine as the
 404 internal standard for human contribution. This discrepancy may be attributed to the dilution effect of non-human
 405 wastewater components, such as industrial and agricultural effluents, which can significantly impact creatinine
 406 concentrations (Choi et al., 2018). In this study, the creatinine levels detected were listed in Supplementary Table 1.
 407 When using pure water as blank, as recommended by the manufacturer, some of our measurements yield negative
 408 values, suggesting the presence of certain interfering substances in wastewater that require further investigation
 409 (Xagorarakis and O'Brien, 2020). As a result, we decided not to use creatinine concentrations to normalize our viral
 410 load data, as the low levels of creatinine detected in our samples might not accurately reflect the human contribution
 411 to the wastewater.

412 To investigate the correlation between the measured viral load in wastewater and the reported COVID-19
 413 cases in El Paso, TX, available viral load data from Haskell Street Wastewater Plant which serves the central and
 414 east area of El Paso were collated with the corresponding daily COVID-19 case counts on the wastewater sample
 415 collection dates in the city covering zip codes 79901, 79902, 79903, 79904, 79905, 79907, 79912, 79915, 79922,
 416 79925, 79928, 79930, 79935, 79936, and 79938. The data was tested for normality using the Shapiro-Wilk test.
 417 Since $p < 0.05$, it was concluded that the data was not normally distributed. Given the small sample size, a non-
 418 parametric test was chosen instead of a parametric test (de Souza et al., 2023; King and Eckersley, 2019). The
 419 Spearman rank correlation test was applied to evaluate the association between the total viral load and the total
 420 number of reported cases on each date across the studied areas. The Spearman rank test is a non-parametric method
 421 that uses the correlation coefficient rho (ρ) to measure the strength and direction of a monotonic relationship
 422 between two variables, with values ranging from -1 (perfect negative correlation) to 1 (perfect positive correlation).
 423 The Spearman correlation coefficient was calculated to assess the relationship between mean virus concentrations

424 and total COVID-19 case counts in the datasets. Due to the unavailability of active case numbers during the early
425 stages of the pandemic (April 2020 to May 2020), the analysis was conducted using cumulative case numbers.
426 During this period, the difference between active and cumulative cases was likely minimal. Additionally, prior
427 studies have indicated that recovered patients may continue shedding the virus (Kampen et al., 2021). During the
428 early period, the analysis revealed a moderate negative correlation of -0.072 between the freeze-dried viral load and
429 the cumulative case numbers. However, this correlation was not statistically significant ($p=0.808$). Similarly, for the
430 ultrafiltration method, using data from the same period, the analysis showed a moderate negative correlation of -
431 0.316 between the viral load and the cumulative COVID-19 case numbers, which was also not statistically
432 significant ($p=0.270$).

433 **4. Discussion**

434 Specific precautions must be followed to mitigate RNA degradation in concentrated wastewater and
435 preserve its integrity for potential future analyses. Immediate sample processing post-collection is ideal for
436 maximizing RNA extraction yield and maintaining its integrity. However, logistical constraints often necessitate
437 sample storage, for which TRIzol or similar denaturing reagents are highly recommended. TRIzol effectively
438 inhibits RNase activity, thereby preventing RNA degradation (Chomczynski and Sacchi, 2006). Concentrated
439 samples in TRIzol demonstrate superior stability for long-term storage, particularly when stored at -80°C freezer
440 (Fabre et al., 2014). Thus, maintaining samples in TRIzol without RNA extraction until imminent RT-qPCR analysis
441 is considered the optimal storage strategy. Moreover, minimizing freeze-thaw cycles of samples, regardless of the
442 storage method, is critical to prevent RNA degradation. RNases are prevalent and can regain enzymatic activity after
443 removing denaturing conditions (Thatcher, 2015). Consequently, after RNA is extracted from the TRIzol storage
444 solution, downstream procedures should be performed promptly to minimize RNA degradation and ensure the
445 reliability and accuracy of the subsequent RT-qPCR analyses.

446 The two concentrating methods demonstrated contrasting advantages and disadvantages. For the
447 pretreatment step, ultrafiltration requires centrifugation and filtration to remove larger solid particles (sewage
448 sludge) that may clog the concentrator. Both steps may result in the loss of viral signals, as evidenced by the signal
449 detection in the pellet collected during the pretreatment steps (Supplementary Table 4). Other studies have also
450 observed a reduction in viral detection after removing solids from wastewater (Ahmed et al., 2020). Accordingly,
451 some studies recommend retaining solids in the wastewater for analysis. In contrast, the freeze-drying method does
452 not involve pretreatment steps to remove solids. All solids are retained in the final concentrate, allowing RNA from
453 these solids to be extracted. However, the freeze-drying method does require an initial overnight low-temperature
454 freezing step (-80°C), which can be time-consuming. Considering that most wastewater samples are pasteurized and
455 stored at -80°C rather than being processed on the same day of collection, this freezing step could also provide
456 flexibility for both sample storage and processing time.

457 For the concentrating process, ultrafiltration involves using expensive filters and multiple centrifugation
458 and liquid handling steps. These steps prolong operator exposure to wastewater, increasing the potential risk of
459 pathogen transmission. Consequently, ultrafiltration requires rigorous personal protective equipment (PPE) and
460 extensive decontamination procedures for centrifuges, rotors, and buckets. This makes the process labor-intensive,
461 thus limiting the throughput to approximately eight samples per day. Contrariwise, the freeze-drying method only
462 uses inexpensive sample bottles. It minimizes operator exposure to wastewater, with only brief handling required for
463 cap loosening of the bottles and mounting the Fast-Freeze Flask (Fig. 1). Decontamination was only needed at the
464 end of the freeze-drying process. Although the freeze-drying method does require three days to concentrate eight
465 samples to the desired volume, it demands minimal labor and reduces exposure to wastewater. Furthermore, the
466 whole process for freeze drying does not require extensive training such as aliquoting and transferring wastewater
467 safely in BSC in ultrafiltration technique (Section 2.3)

468 Detection sensitivity is a critical factor in evaluating concentrating methods. The higher detection
469 sensitivity of the freeze-drying method can be attributed to several potential factors. Firstly, as literature
470 demonstrated, many viruses can be associated with sewage sludge (Kitajima et al., 2020; Ye et al., 2016). By
471 retaining all components of the wastewater, freeze-drying maximizes the capture of viruses present in wastewater. In
472 contrast, ultrafiltration may exclude viral particles bound to sewage sludge, potentially resulting in signal loss.
473 Secondly, the freeze-drying process involves fewer liquid handling steps and minimizes sample loss during
474 processing, further contributing to its higher detection efficiency. Additionally, the cryogenic environment
475 maintained during freeze-drying helps prevent RNA degradation, preserving the integrity of viral genetic material
476 for downstream detection. The freeze-drying method's higher detection ratio and lower detection limit highlight its
477 advantages for early detection of viral pathogens during the onset of a pandemic. By effectively capturing and

478 concentrating viral material from wastewater samples, freeze-drying facilitates the identification of emerging viral
479 threats at lower prevalence levels, enabling the timely implementation of public health interventions and
480 surveillance strategies.

481 The relationship between wastewater viral load and community COVID-19 cases is a key consideration in
482 evaluating the utility of wastewater surveillance. Our finding is consistent with the literature, which has reported
483 varying degrees of correlation between wastewater viral loads and community-level COVID-19 cases. Several
484 studies have demonstrated a positive correlation, with higher viral loads in wastewater preceding or coinciding with
485 increased case counts in the corresponding communities (Medema et al. 2020; Randazzo et al. 2020). However,
486 other studies have reported weaker or inconsistent correlations, potentially due to factors such as varying viral
487 shedding patterns, differences in testing rates, and the influence of local conditions on viral transport and persistence
488 in wastewater systems (Gonzalez et al. 2020). It is important to note that the correlation observed in this study is
489 based on minimal data from the early stages of the pandemic and lacks reliable normalization of human contribution
490 to wastewater. Although this study's primary focus is the evaluation and comparison of the freeze-drying and
491 ultrafiltration methods for concentrating viral particles from wastewater samples, the correlation analysis still
492 offered some insights into the relationship between wastewater viral loads and community-level case counts.

493 In summary, this study demonstrated that the freeze-drying method outperforms the widely used
494 ultrafiltration technique for concentrating viral particles from wastewater samples. The freeze-drying approach
495 exhibited higher overall recovery rates for the surrogate virus OC43, a higher detection ratio for SARS-CoV-2 viral
496 RNA, and lower detection limits, particularly during the early stages of the COVID-19 pandemic. These findings
497 highlight the superior ability of freeze-drying to capture and retain viral material from complex wastewater matrices.
498 While freeze-drying is more time-consuming, it offers several advantages over ultrafiltration. It eliminates the need
499 for pretreatment steps that might exclude viral signals associated with sewage sludge. Additionally, freeze-drying
500 provides flexibility in sample storage, reduces labor demands and exposure risks, and requires minimum training.
501 These advantages make freeze-drying a favorable option for wastewater virus detection, especially in resource-
502 constrained settings such as wastewater treatment facilities with limited personnel and training resources.
503 Combining efficient viral particle capture and operational practicality, positions freeze-drying as a promising
504 approach for enhancing community-level early warning and surveillance capabilities against emerging viral threats.
505

506 **Statement:**

507 During the preparation of this work, the author(s) utilized ChatGPT to enhance readability and improve language.
508 Following its use, the authors carefully reviewed and edited the content as necessary and took full responsibility for
509 the final version of the publication.

510 **Acknowledgements:**

511 The authors would like to acknowledge Teresa T. Alcala and El Paso Water Laboratory personnel: Hugo Ruiz at
512 John T. Hickerson Water Reclamation Facility, Martin L. Ortiz at Roberto Bustamante Wastewater Plant, Rick
513 Dominguez at Haskell Street Wastewater Plant, Roberto Hernandez at Fred Hervey Water Reclamation, for their
514 assistance during wastewater sample collection especially during the COVID-19 pandemic period. This work
515 received funding from the College of Science, University of Texas at El Paso. The work has used instruments in the
516 Border Biomedical Research Center (BBRC) that is supported by the National Institutes on Minority Health and
517 Health Disparities (NIMHD) of the National Institutes of Health (NIH) under award number U54MD007592.
518 Special thanks go to BBRC personnel Georgialina Rodriguez and Ana P. Betancourt who helped us use the
519 instruments. RD and CX also received support from the National Institute of General Medical Sciences (NIGMS) of
520 NIH under award number R01GM129525 and from the Welch Foundation under Grant Number AH-2126-
521 20220331. WYL received support from NIGMS of NIH under award number SC1CA245675. The content is solely
522 the responsibility of the authors and does not necessarily represent the official views of the funding agencies.
523
524

525 Reference:

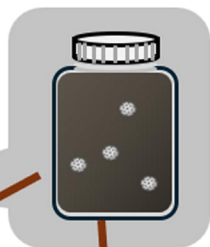
- 526
- 527 Ahmed W, Bertsch PM, Bibby K, Haramoto E, Hewitt J, Huygens F, et al. Decay of SARS-CoV-2 and surrogate murine hepatitis virus RNA in
528 untreated wastewater to inform application in wastewater-based epidemiology. *Environmental Research* 2020; 191: 110092.
- 529 Bustin SA, Benes V, Garson JA, Hellemans J, Huggett J, Kubista M, et al. The MIQE guidelines: minimum information for publication of
530 quantitative real-time PCR experiments. *Clinical Chemistry* 2009; 55: 611-622.
- 531 CDC. Interim Laboratory Biosafety Guidelines for Handling and Processing Specimens Associated with Coronavirus Disease 2019 (COVID-19).
532 Centers for Disease Control and Prevention. 2020a; 2020/2/11/ [https://www.cdc.gov/coronavirus/2019-ncov/lab/lab-biosafety-](https://www.cdc.gov/coronavirus/2019-ncov/lab/lab-biosafety-guidelines.html)
533 [guidelines.html](https://www.cdc.gov/coronavirus/2019-ncov/lab/lab-biosafety-guidelines.html)
- 534 CDC. Number of COVID-19 deaths reported to WHO (cumulative total). Centers for Disease Control and Prevention. 2020b; Last Update on
535 12/15/2024. <https://data.who.int/dashboards/covid19/deaths>
- 536 Chen Y, Senesi N, Schnitzer M. Information Provided on Humic Substances by E4/E6 Ratios. *Soil Science Society of America Journal* 1977; 41:
537 352-358.
- 538 Choi PM, Tschärke BJ, Donner E, O'Brien JW, Grant SC, Kaserzon SL, et al. Wastewater-based epidemiology biomarkers: Past, present and
539 future. *TrAC Trends in Analytical Chemistry* 2018; 105: 453-469.
- 540 Chomczynski P, Sacchi N. The single-step method of RNA isolation by acid guanidinium thiocyanate-phenol-chloroform extraction: twenty-
541 something years on. *Nature Protocols* 2006; 1: 581-585.
- 542 Damian Riina M, Stambaugh C, Stambaugh N, Huber KE. Chapter 28 - Continuous variable analyses: t-test, Mann-Whitney, Wilcoxon rank. In:
543 Eltorai AEM, Bakal JA, Kim DW, Wazer DE, editors. *Translational Radiation Oncology*. Academic Press, 2023, pp. 153-163.
- 544 Dare RK, Fry AM, Chittaganpitch M, Sawanpanyalert P, Olsen SJ, Erdman DD. Human coronavirus infections in rural Thailand: a
545 comprehensive study using real-time reverse-transcription polymerase chain reaction assays. *J Infect Dis* 2007; 196: 1321-8.
- 546 Daughton CG. Real-time estimation of small-area populations with human biomarkers in sewage. *The Science of the Total Environment* 2012;
547 414: 6-21.
- 548 de Souza RR, Toebe M, Mello AC, Bittencourt KC. Sample size and Shapiro-Wilk test: An analysis for soybean grain yield. *European Journal of*
549 *Agronomy* 2023; 142.
- 550 Fabre A-L, Colotte M, Luis A, Tuffet S, Bonnet J. An efficient method for long-term room temperature storage of RNA. *European Journal of*
551 *Human Genetics* 2014; 22: 379-385.
- 552 Farkas K, Hillary LS, Malham SK, McDonald JE, Jones DL. Wastewater and public health: the potential of wastewater surveillance for
553 monitoring COVID-19. *Current Opinion in Environmental Science & Health* 2020; 17: 14-20.
- 554 Fontenele RS, Kraberger S, Hadfield J, Driver EM, Bowes D, Holland LA, et al. High-throughput sequencing of SARS-CoV-2 in wastewater
555 provides insight into circulating variants. *Water Research* 2021; 205: 117710.
- 556 Friedler E, Butler D, Alfiya Y. Wastewater composition. In: Larsen TA, Udert KM, Lienert J, editors. *Source Separation and Decentralization for*
557 *Wastewater Management*, 2013, pp. 240-257.
- 558 Henze M. *Biological wastewater treatment: principles, modelling and design*. London: IWA Pub., 2008.
- 559 Hughes J, Cowper-Heays K, Olesson E, Bell R, Stroombergen A. Impacts and implications of climate change on wastewater systems: A New
560 Zealand perspective. *Climate Risk Management* 2021; 31: 100262.
- 561 Kampen JJA, Vijver DAMC, Fraaij PLA, Haagmans BL, Lamers MM, Okba N, et al. Duration and key determinants of infectious virus shedding
562 in hospitalized patients with coronavirus disease-2019 (COVID-19). *Nature Communications* 2021; 12: 267.
- 563 Katukiza AY, Ronteltap M, Niwagaba CB, Foppen JWA, Kansime F, Lens PNL. Sustainable sanitation technology options for urban slums.
564 *Biotechnology Advances* 2012; 30: 964-978.
- 565 King AP, Eckersley RJ. Chapter 7 - Inferential Statistics IV: Choosing a Hypothesis Test. In: King AP, Eckersley RJ, editors. *Statistics for*
566 *Biomedical Engineers and Scientists*. Academic Press, 2019, pp. 147-171.
- 567 Kitajima M, Ahmed W, Bibby K, Carducci A, Gerba CP, Hamilton KA, et al. SARS-CoV-2 in wastewater: State of the knowledge and research
568 needs. *The Science of the Total Environment* 2020; 739: 139076.
- 569 Liu B, Zhou X. Freeze-Drying of Proteins. In: Wolkers WF, Oldenhof H, editors. *Cryopreservation and Freeze-Drying Protocols*. Springer, New
570 York, NY, 2015, pp. 459-476.
- 571 Lu X, Wang L, Sakthivel SK, Whitaker B, Murray J, Kamili S, et al. US CDC Real-Time Reverse Transcription PCR Panel for Detection of Severe
572 Acute Respiratory Syndrome Coronavirus 2. *Emerging Infectious Diseases* 2020; 26: 1654-1665.
- 573 Medema G, Heijnen L, Elsinga G, Italiaander R, Brouwer A. Presence of SARS-Coronavirus-2 RNA in sewage and correlation with reported
574 COVID-19 prevalence in the early stage of the epidemic in the Netherlands. *Environmental Science & Technology Letters* 2020.
- 575 Otterpohl R, Buzie C. Treatment of the solid fraction. In: Larsen TA, Udert KM, Lienert J, editors. *Source Separation and Decentralization for*
576 *Wastewater Management*, 2013, pp. 258-273.
- 577 Patterson EI, Prince T, Anderson ER, Casas-Sanchez A, Smith SL, Cansado-Utrilla C, et al. Methods of Inactivation of SARS-CoV-2 for
578 Downstream Biological Assays. *The Journal of Infectious Diseases* 2020; 222: 1462-1467.
- 579 Prot T, Korving L, Van Loosdrecht MCM. Ionic strength of the liquid phase of different sludge streams in a wastewater treatment plant. *Water*
580 *Sci Technol* 2022; 85: 1920-1935.
- 581 Qin C, Chen C, Shang C, Xia K. Fe³⁺-saturated montmorillonite effectively deactivates bacteria in wastewater. *Science of The Total*
582 *Environment* 2018; 622-623: 88-95.
- 583 Rashid R, Shafiq I, Akhter P, Iqbal MJ, Hussain M. A state-of-the-art review on wastewater treatment techniques: the effectiveness of adsorption
584 method. *Environ Sci Pollut Res Int* 2021; 28: 9050-9066.
- 585 RStudio Team. RStudio: Integrated Development for R. RStudio, PBC, Boston, MA. 2020; Last Update on [https://support.posit.co/hc/en-](https://support.posit.co/hc/en-us/articles/206212048-Citing-RStudio)
586 [us/articles/206212048-Citing-RStudio](https://support.posit.co/hc/en-us/articles/206212048-Citing-RStudio)
- 587 Rusiñol M, Zammit I, Itarte M, Forés E, Martínez-Puchol S, Girones R, et al. Monitoring waves of the COVID-19 pandemic: Inferences from
588 WWTPs of different sizes. *Science of The Total Environment* 2021; 787: 147463.
- 589 Sahu O, Mazumdar B, Chaudhari PK. Treatment of wastewater by electrocoagulation: a review. *Environ Sci Pollut Res Int* 2014; 21: 2397-413.
- 590 Shi W, Zhuang WE, Hur J, Yang L. Monitoring dissolved organic matter in wastewater and drinking water treatments using spectroscopic
591 analysis and ultra-high resolution mass spectrometry. *Water Res* 2021; 188: 116406.
- 592 Svec D, Tichopad A, Novosadova V, Pfaffl MW, Kubista M. How good is a PCR efficiency estimate: Recommendations for precise and robust
593 qPCR efficiency assessments. *Biomolecular Detection and Quantification* 2015; 3: 9-16.

594 Taylor SC, Laperriere G, Germain H. Droplet Digital PCR versus qPCR for gene expression analysis with low abundant targets: from variable
595 nonsense to publication quality data. *Scientific Reports* 2017; 7: 2409.
596 Thatcher SA. DNA/RNA preparation for molecular detection. *Clinical Chemistry* 2015; 61: 89-99.
597 Wakefield JH. Understanding Separation Essentials For Wastewater Treatment. *Water Online*. 2015; Last Update on 05/15/2015.
598 <https://www.wateronline.com/doc/understanding-separation-essentials-for-wastewater-treatment-0001>
599 Weißbecker C, Buscot F, Wubet T. Preservation of nucleic acids by freeze-drying for next generation sequencing analyses of soil microbial
600 communities. *Journal of Plant Ecology* 2017; 10: 81-90.
601 World Health Organization W. Coronavirus disease (COVID-19): situation report, 158. World Health Organization, 2020.
602 Wurtzer S, Marechal V, Mouchel JM, Maday Y, Teyssou R, Richard E, et al. Evaluation of lockdown effect on SARS-CoV-2 dynamics through
603 viral genome quantification in waste water, Greater Paris, France, 5 March to 23 April 2020. *Eurosurveillance* 2020; 25: 2000776.
604 Xagorarakis I, O'Brien E. Wastewater-Based Epidemiology for Early Detection of Viral Outbreaks. In: O'Bannon DJ, editor. *Women in Water*
605 *Quality: Investigations by Prominent Female Engineers*. Springer International Publishing, Cham, 2020, pp. 75-97.
606 Ye Y, Ellenberg RM, Graham KE, Wigginton KR. Survivability, Partitioning, and Recovery of Enveloped Viruses in Untreated Municipal
607 Wastewater. *Environmental Science & Technology* 2016; 50: 5077-5085.
608 Zhang S, Li X, Wu J, Coin L, O'Brien J, Hai F, et al. Molecular Methods for Pathogenic Bacteria Detection and Recent Advances in Wastewater
609 Analysis. *Water* 2021; 13: 3551.
610
611

Wastewater Treatment Plant



Sample Collection

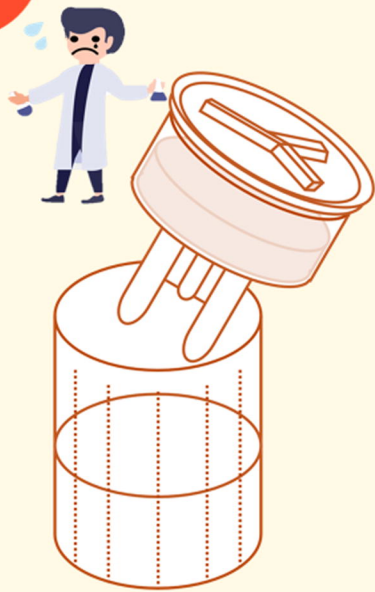
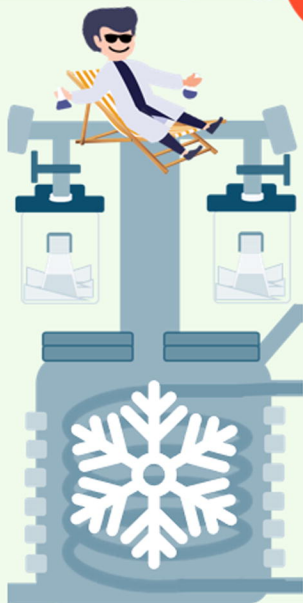


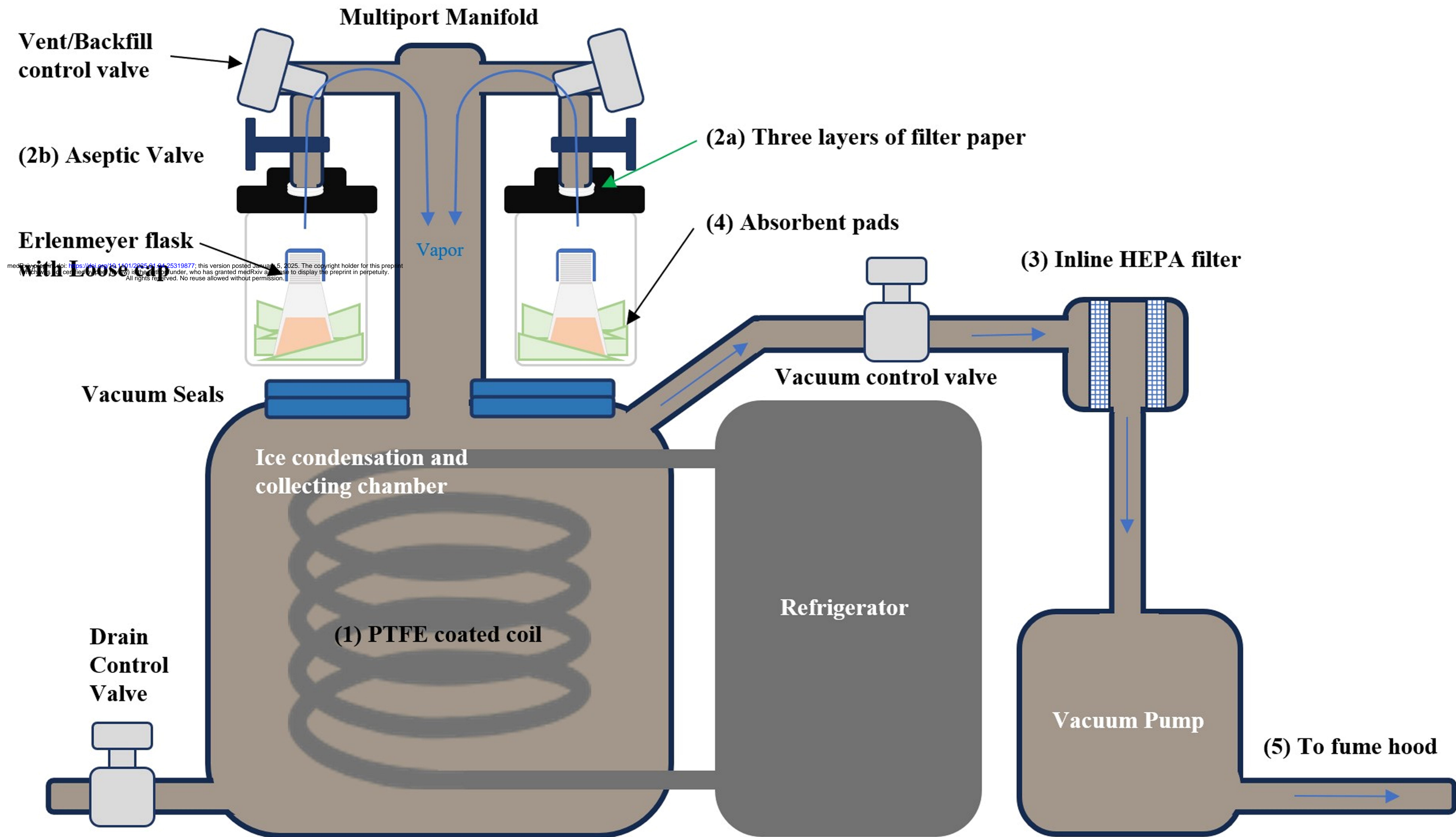
Virus concentrating

Freeze drying

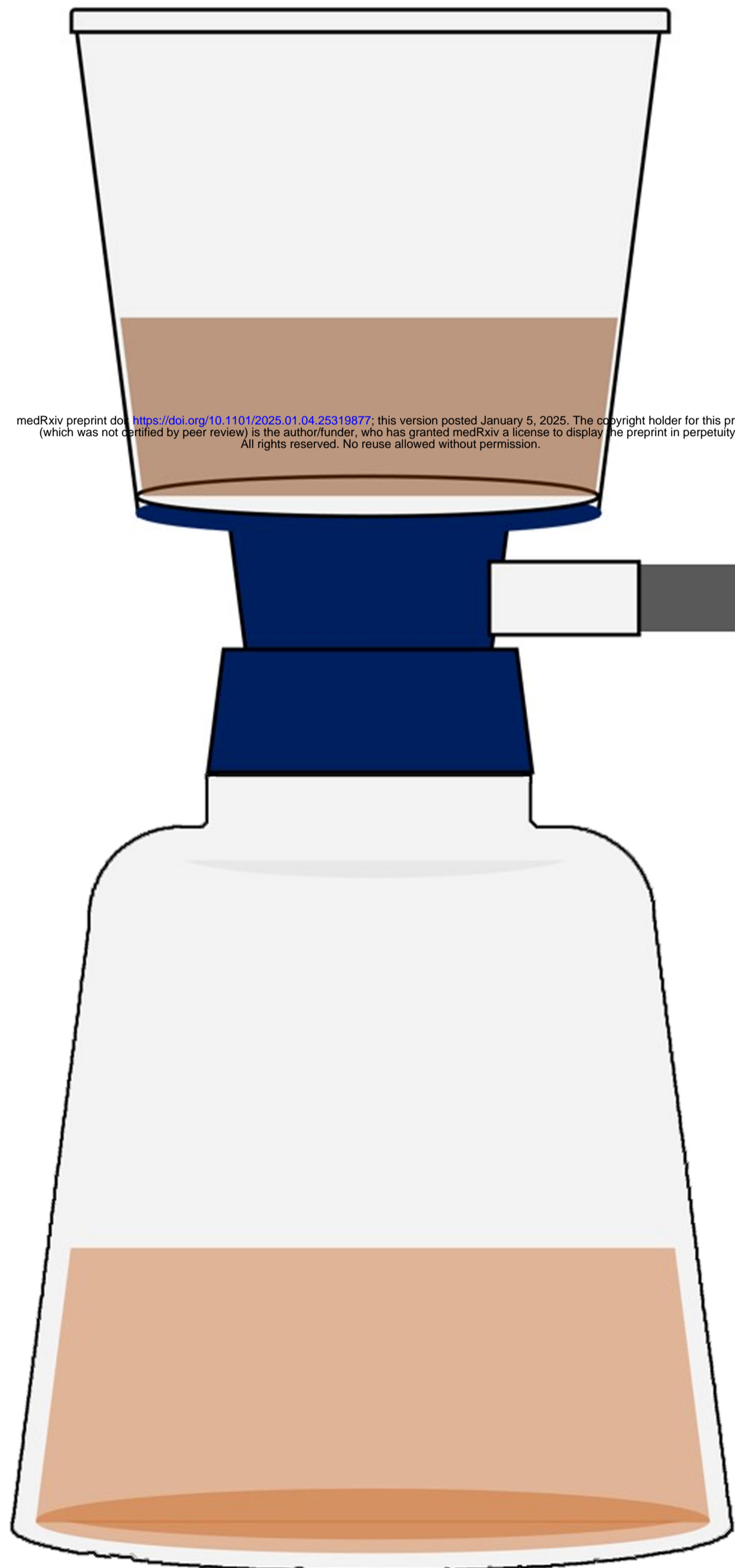
VS

Ultrafiltration





0.22 μ m PES bottle filter



medRxiv preprint doi: <https://doi.org/10.1101/2025.01.04.25319877>; this version posted January 5, 2025. The copyright holder for this preprint (which was not certified by peer review) is the author/funder, who has granted medRxiv a license to display the preprint in perpetuity. All rights reserved. No reuse allowed without permission.

Inside BSC

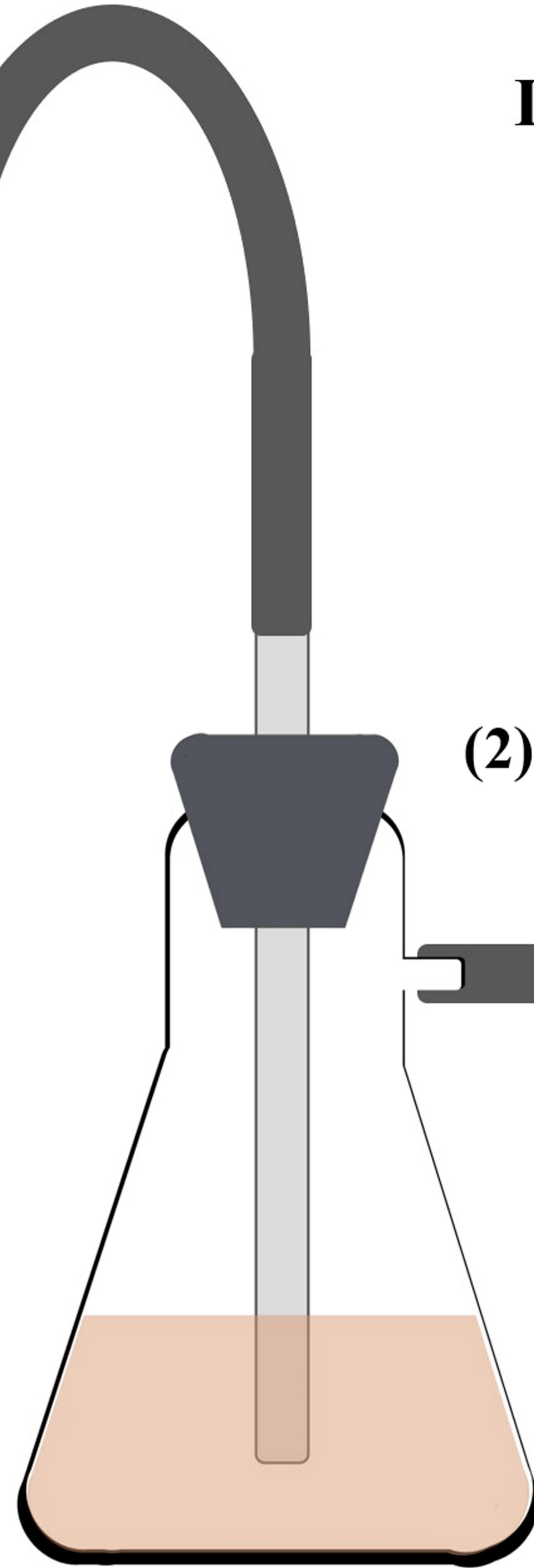
(2) In-line 0.22 μ m filter



Vacuum control valve

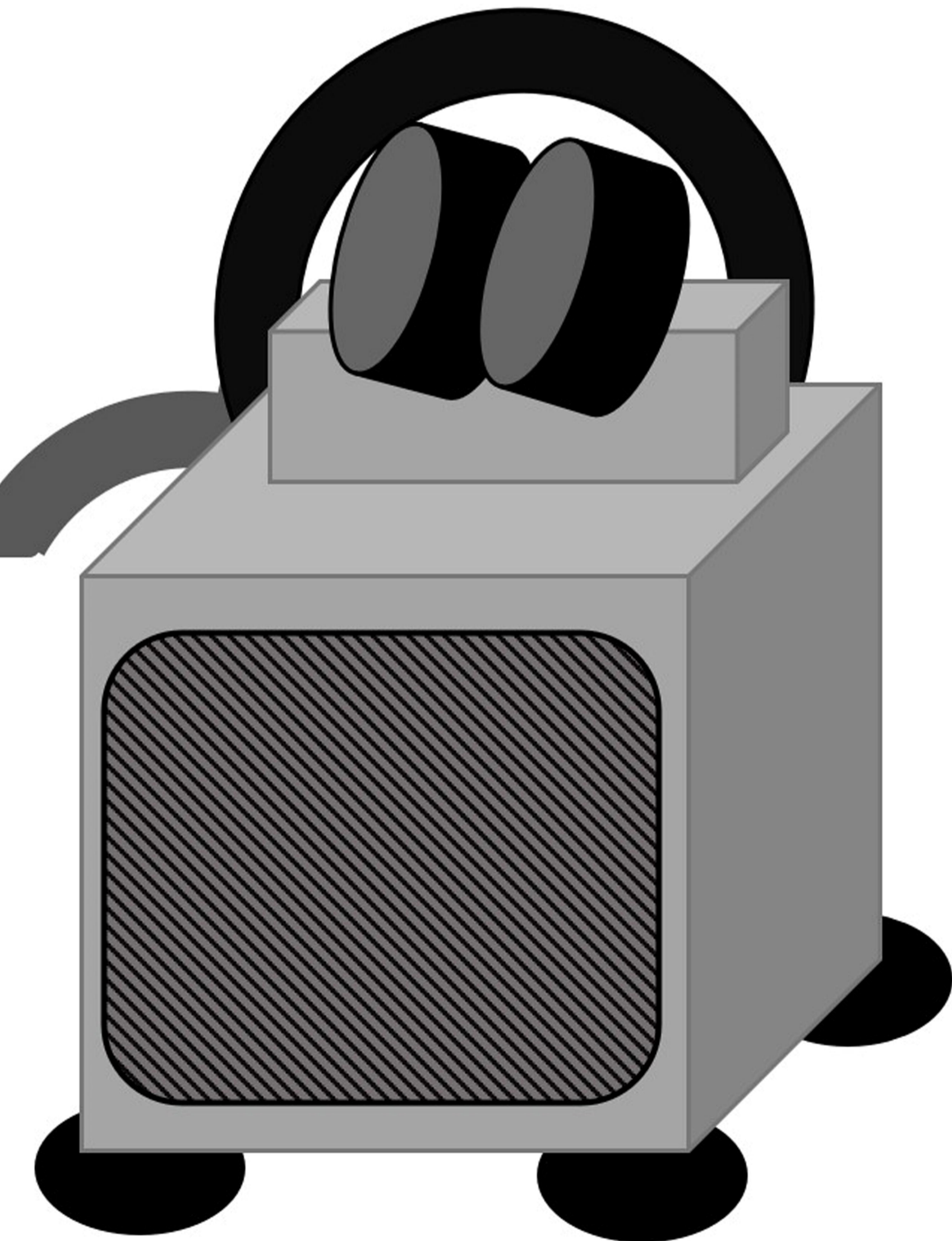


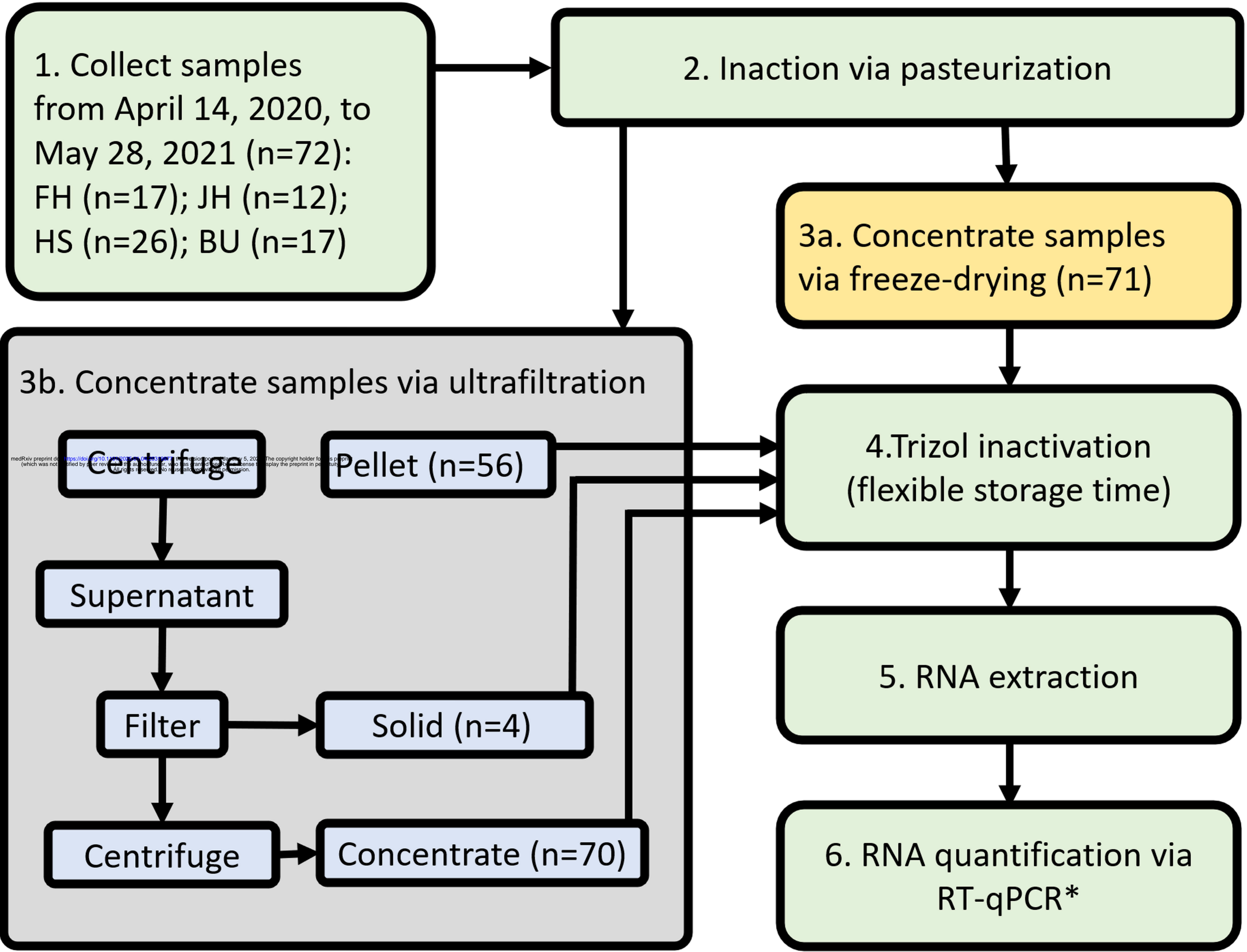
(1) Trap bottle with disinfectant



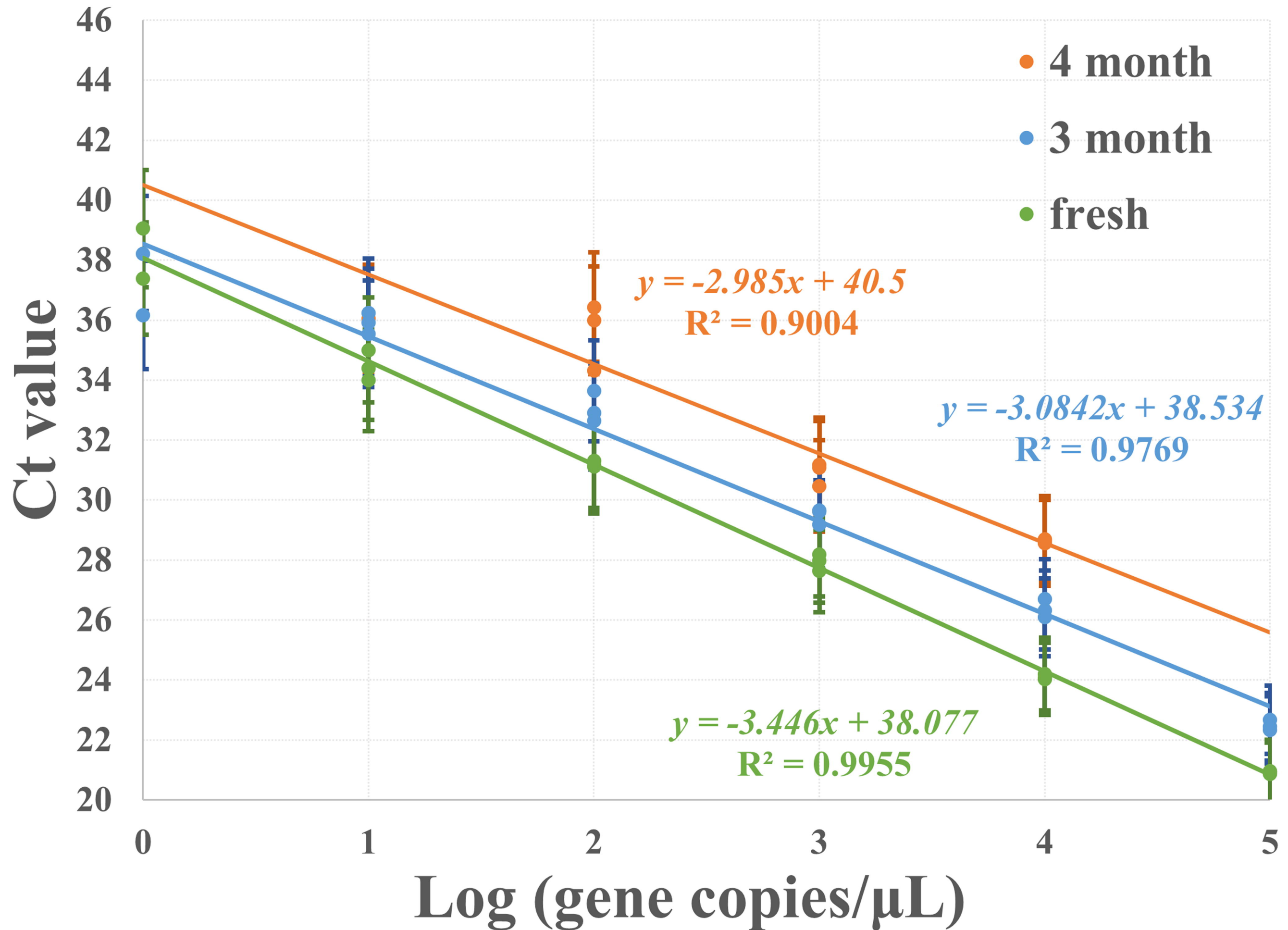
Outside BSC

Vacuum pump

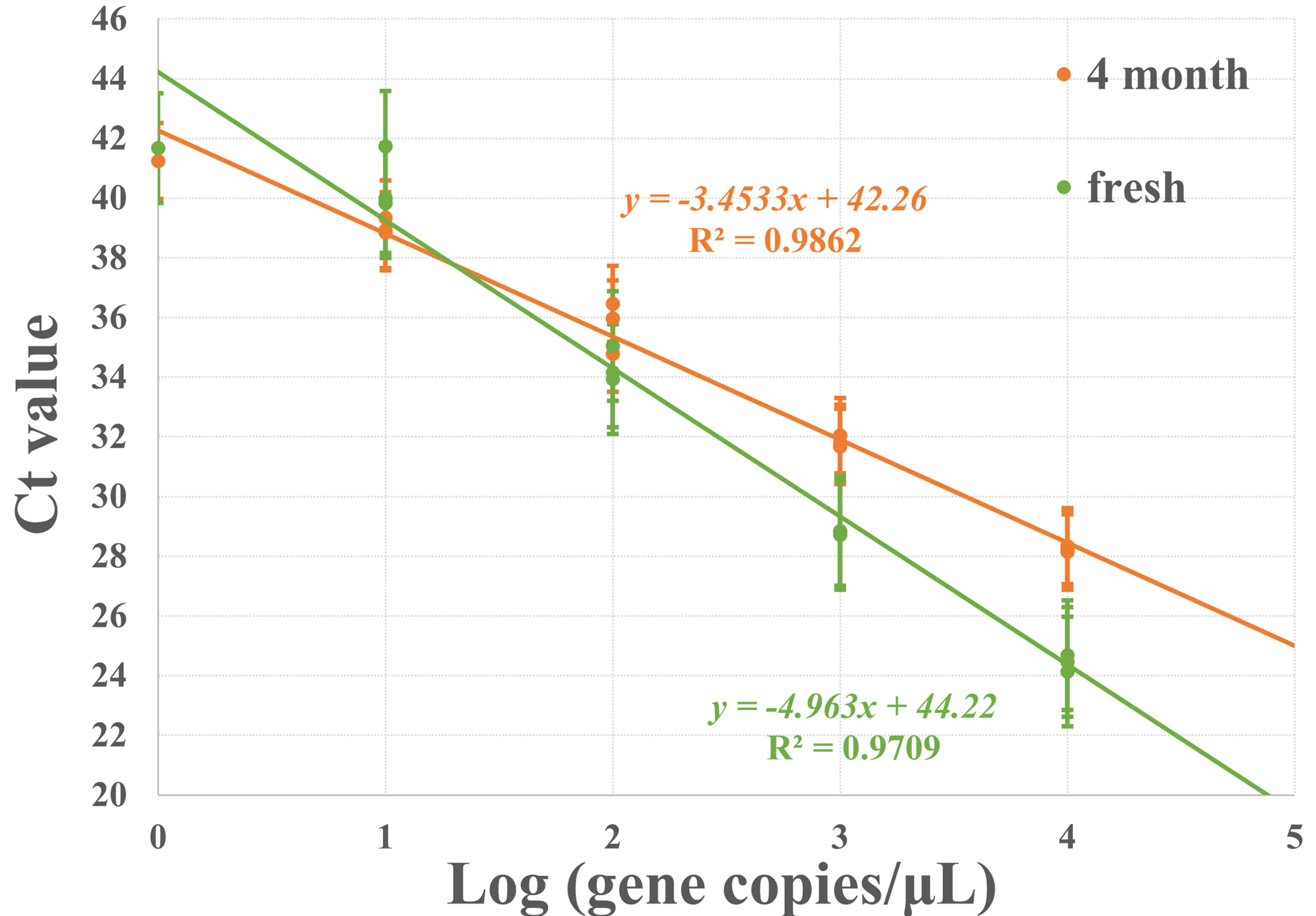




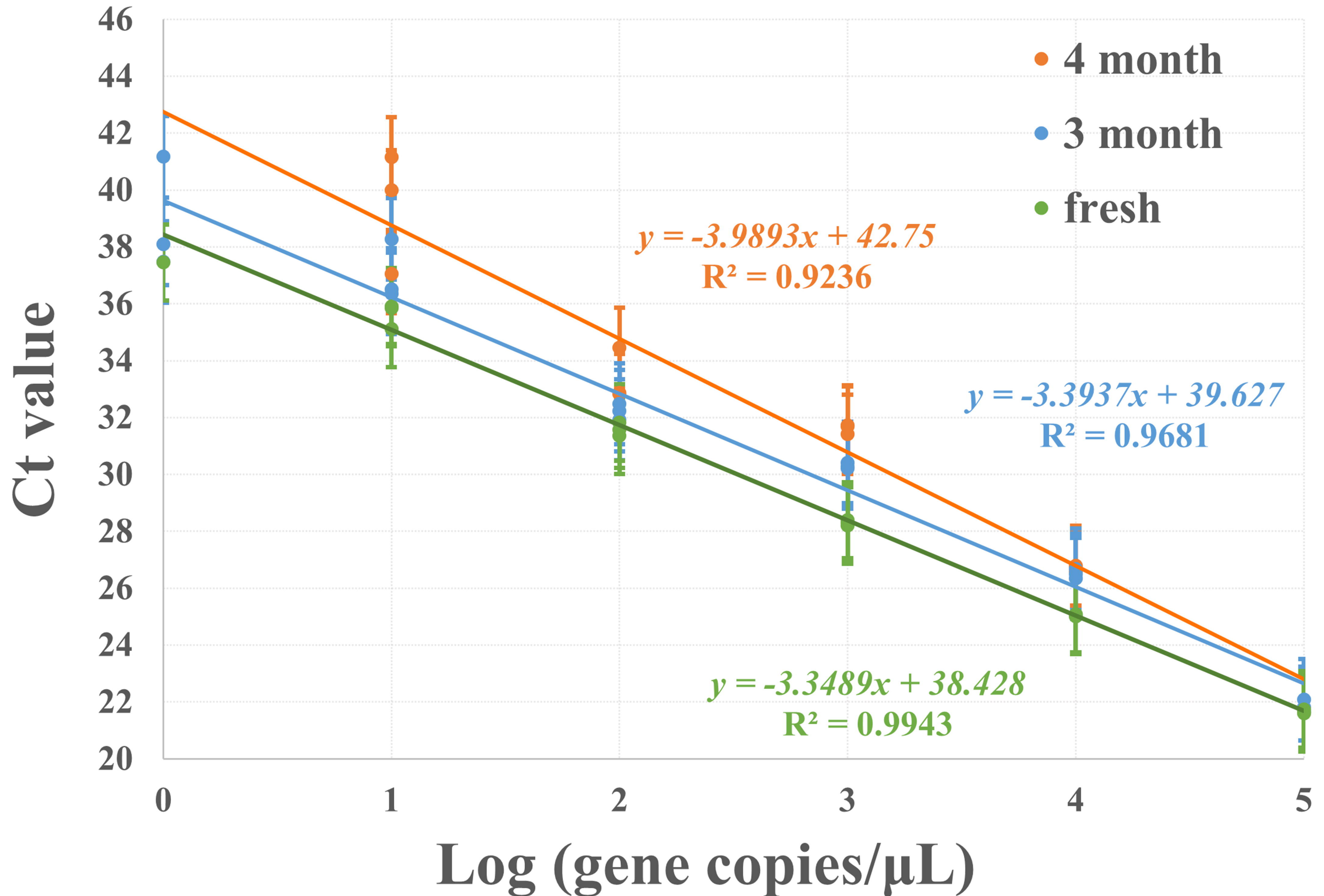
A. RNA standard curves (N1 assay)



B. RNA standard curves (N2 assay)



C. DNA standard curves (N1 assay)



D. DNA standard curves (N2 assay)

